

Issued by Sandia National Laboratories, operated for the United States Department of Energy by Sandia Corporation.

NOTICE: This report was prepared as an account of work sponsored by an agency of the United States Government. Neither the United States Government nor any agency thereof, nor any of their employees, nor any of their contractors, subcontractors, or their employees, makes any warranty, express or implied, or assumes any legal liability or responsibility for the accuracy, completeness, or usefulness of any information, apparatus, product, or process disclosed, or represents that its use would not infringe privately owned rights. Reference herein to any specific commercial product, process, or service by trade name, trademark, manufacturer, or otherwise, does not necessarily constitute or imply its endorsement, recommendation, or favoring by the United States Government, any agency thereof or any of their contractors or subcontractors. The views and opinions expressed herein do not necessarily state or reflect those of the United States Government, any agency thereof or any of their contractors or subcontractors.

SAND84-2548
Internal Distribution Only
Printed April 1985

A Study of the Perforation of Widely Spaced Metal Plates

A. Keith Miller
Advanced Systems Division I
Fred J. Zeigler
Computational Physics and Mechanics Division I
Sandia National Laboratories
Albuquerque, NM 87185

Abstract

The use of high-velocity metal rods to penetrate multiple, spaced plates of armor is being investigated for potential weapon systems applications. Two computational models were developed and a perforation test was performed to assess the initial performance of this concept as a basis for further development.

in dia, 17.5 in. long (L/D ratio of 19), and weighed 9.3 lb. The penetrator's aluminum windshield and hardened, sharp steel point were removed to allow the blunted end of the penetrator to first contact the target plates.

The target array was positioned 300 ft from the gun to allow the sabot to be air-stripped before reaching the target. A series of vertical cardboard cards (yaw cards) were positioned at 10-ft intervals in front of the first plate of the target array to measure the attitude of the penetrator as it approached the target. The three cards closest to the target array contained conductive grids which, when broken by the penetrator, activated timing circuits to measure the velocity of the penetrator before impact with the first plate.

Six high-speed motion picture cameras and two image motion cameras were trained on the target, as shown in Figure 1, to obtain velocity data and to determine the attitude of the penetrator as it progressed through the target array. Although the test yielded good film records, excessive debris obscured the penetrator so no velocity data were obtained after impact with the first plate.

HULL Simulation of the Experiment

The experiment described above was modeled with a HULL computation, restricted to the perforation of the first plate. Fins were not included as part of the penetrator, which was modeled as a cylinder.

Figure 2 shows the oblique impact angle between the penetrator and target just before impact. The section shown lies in the x-z plane with the y-axis coming vertically out of the page (so that $y = 0$ in the figure).

A three-dimensional computation of the problem was done on a $36 \times 18 \times 128$ x-y-z grid. From the initial setup of Figure 2 the calculation was run in the reverse ballistic mode, with the plate moving toward the stationary penetrator at 5300 fps (the intended experimental velocity of the penetrator).

The HULL hydrocode produces approximate solutions to the partial differential equations of continuum mechanics. These equations represent the conservation of mass, momentum, and energy for each of the materials in the problem. Additionally, equations of state, along with certain material properties,

must be implemented for each material to determine the stress as a function of the strain. In HULL, viscous effects are not included in the physics.

The equations of motion are solved in finite difference form. Thus, the differential equations discussed above, which are valid for all points in space, are replaced by a set of algebraic finite difference equations, valid at the grid points. Given the values of the density, energy, velocities, and stress for each material at each grid point at a certain time, the problem is then advanced to the next time value by solving the finite difference equations.

The penetrator was modeled as pure tungsten, with a yield strength of 290 000 psi and a density of 0.65 lb/in³. For RHA we assumed a yield strength of 217 500 psi with a density of 0.28 lb/in³.

A useful relationship that determines the strain field in the impacting materials is the relationship between the shock speed in the material, the particle speed, and the sound (elastic strain wave) speed. This relationship is $U_s = C_o + S U_p$, where U_s is the shock wave speed, C_o is the sonic velocity, and U_p is the particle velocity. The instantaneous particle velocity is a function of the pressure field. The sound speed and the empirically determined constant, S , are considered material parameters. For tungsten, $C_o = 1.57 \times 10^5$ in./s, $S = 1.27$. For the RHA, $C_o = 1.82 \times 10^5$ in./s, $S = 1.73$.

To compute the yaw rate after perforation, it was necessary to compute the angular momentum of the remaining part of the penetrator. Cells that contained tungsten that was separated from the main mass of the penetrator were discarded. The angular momentum of the tungsten in the remaining cells around the center of mass was computed, then summed over all the cells to get the final result. The moment of inertia was computed in a similar way, then these two numbers were used to compute the angular velocity (yaw rate).

Density plots of various stages of the calculation are presented in Figure 3, views (a) through (d). The contours shown are curves of constant density, with values of the density ranging from 0.09 to 0.62 lb/in³. The curves indicate the outlines of the different material shapes in the configuration. As shown in the plots, the diameter of the hole is about 2-2/3 times as large as the original diameter of the penetrator.

A few results are summarized in Table 1. The quantities given refer to the penetrator.

Table 1. HULL Computation Results for Impact of the First Plate

| | Initial | Exiting First Plate |
|----------------|---------|---------------------|
| Velocity (fps) | 5300 | 4550 |
| Weight (lb) | 5.764 | 5.104 |
| Length (in.) | 17.75 | 11 |
| Yaw rate (°/s) | 0 | 5000* |

*Toward the normal axis of the plate

For further information about the HULL code, see Reference 1.

DRI Engineering Model Simulation of the Experiment

The engineering model formulated at the Denver Research Institute can be used to calculate the residual mass, velocity, and attitude of a penetrator as it passes through a series of target plates. This model was exercised to simulate the ballistic test described in Experiment Results.

The features of the DRI model are described in References 2 through 4. A comparison of this model to other ballistic impact models has been performed,⁵ which indicates that this model is probably the most conservative of the models available to date. The comparative results presented show that the method of calculating the ballistic limit velocity and the residual velocity in the DRI model is similar to other methods, although the DRI model adds some empirically derived constants to adjust those values for penetrators that lose mass and change shape.⁴ The method of calculating the mass loss is unique in the DRI model in that it first calculates the mass loss due to erosion while the interface-relative velocity between the target plate and the penetrator is greater than the plastic wave speed in the penetrator. The

model then calculates the additional mass loss of the penetrator caused by extrusion of the nose and subsequent shear of the extrusion lips. This is followed by a calculation to determine whether damaging bending moments are applied to the penetrator for sufficient time to cause the penetrator to break up or shatter.

An empirical relationship predicting the tumble rate of the penetrator as it exits each plate, based on the penetrator impact attitude, length, velocity, and plate thickness, is included in the model.

The pertinent material properties for the target plates are shown in Figure 1. A density of 0.28 lb/in³ was assigned to each of the plates. The properties assigned to the tungsten alloy penetrator are as follows:

| | |
|------------------------------|-------------------------|
| Density | 0.63 lb/in ³ |
| Brinell hardness number | 295 |
| Compressive modulus | 5.30×10^7 psi |
| Static yield strength | 1.27×10^5 psi |
| Dynamic yield strength | 1.68×10^5 psi |
| Strain to failure | 0.29 |
| Percentage reduction of area | 23% |
| Plastic wave velocity | 100 in./s |

The desired initial impact velocity of 5300 fps was not achieved in the test (5150 fps was obtained). However, because no residual velocity information was obtained, the two computational simulations (the HULL model and the DRI model) were not rerun at the actual test impact velocity. The desired impact velocity of 5300 fps was used in both the HULL and DRI models so that the two computations could be compared.

The perforation parameters calculated by the DRI model simulation of the test are shown in Table 2. Note that the initial length, diameter, and weight of the penetrator used in the HULL and DRI model calculations are slightly different than for the penetrator used in the experiment. The calculations were performed before the experiment, using estimates of the penetrator geometry. Since considerable computer time is needed to perform the HULL calculations, and because insufficient information was obtained from the experiment to benchmark the calculations, the same penetrator geometry was used in both sets of calculations, and the HULL calculations were not repeated.

variance is a result of the different methods used to model the perforation events. The DRI model allows only a short distance of the penetrator to extrude to a larger diameter, which is then sheared off by the target plate to a diameter 1.25 times the original penetrator diameter. The rest of the penetrator remains at its original diameter. The HULL model does not incorporate such an arbitrary material loss mechanism and, as can be seen in the density plots of the HULL results, the penetrator extrudes to a larger diameter throughout a large percentage of its length. This accounts for the agreement in length but disagreement in weight.

One of the major reasons for performing the HULL calculations was to check the empirical relationship for the penetrator tumble rate that was used in the DRI model. The agreement in the tumble rates was surprisingly good. The HULL simulation predicted a tumble rate of $5000^\circ/\text{s}$, whereas the DRI model predicted $6140^\circ/\text{s}$.

The diameter of the hole pierced through the first plate (≈ 2.5 in.) was very close to the diameter predictions made in the HULL computations. This indicates that the material displacement process (the pressure and velocity fields) simulated in the HULL computations are in good agreement with the actual process in the perforation event.

Recommendations for Future Work

The major portion of future work should be directed toward obtaining adequate experimental data to benchmark the HULL and DRI simulations. Special emphasis should be placed on obtaining data on the size, attitude, and velocity of the penetrating rod immediately after it exits each plate of the target array. Flash x-ray equipment will provide images of

the main portion of the ballistic penetrators. However, highly accurate timing information is required with the x-ray images to determine the parameters of interest.

We need to develop statistics by repeatedly testing a particular target array at a given set of impact conditions. Several extremes of the possible design space also need to be tested and analyzed by computational simulations. The effects of material models and properties (state equations) on the perforation performance need to be explored in the simulations.

We also need to develop better methods for measuring the damage potential of the dense debris cloud in the ballistic experiments.

In sum, the combined efforts of simulating ballistic experiments and the actual performance of such experiments are necessary to understand, and later to optimize, the perforation of multiple plate target arrays.

References

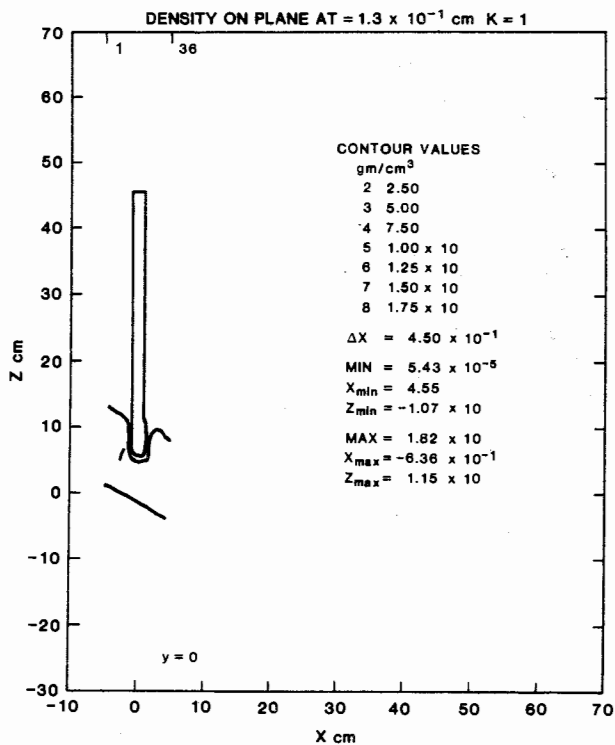
¹D. A. Matuska, *HULL Users Manual*, AFATL-TR-84-59, June 1984.

²Rodney F. Recht and Jerome D. Yatteau, "Multiple Plate Penetration Modeling for Deforming and Yawing Ballistic Penetrators Which Lose Mass," *Seventh International Symposium on Ballistics Proceedings*, The Hague, The Netherlands, 19-21 April 1983, pp 271-80.

³Rodney F. Recht, "Taylor Ballistic Impact Modelling Applied to Deformation and Mass Loss Determinations," *Int J of Eng Sci*, 16:809-27 (1978).

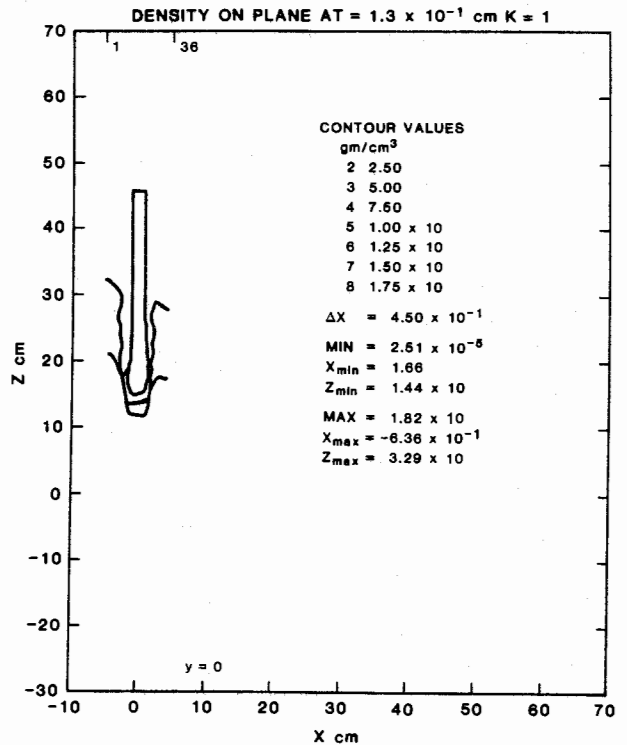
⁴Rodney F. Recht, "Rod Penetration and Component Vulnerability Modeling," private communication with A. K. Miller, Division 1651, Sandia National Laboratories, Albuquerque, NM, 6 September 1983.

⁵A. Keith Miller, *An Evaluation of Three Engineering Models for Predicting the Ballistic Perforation of Multiple Plates by Long Rods*, SAND83-2246 (Albuquerque, NM: Sandia National Laboratories, March 1983).



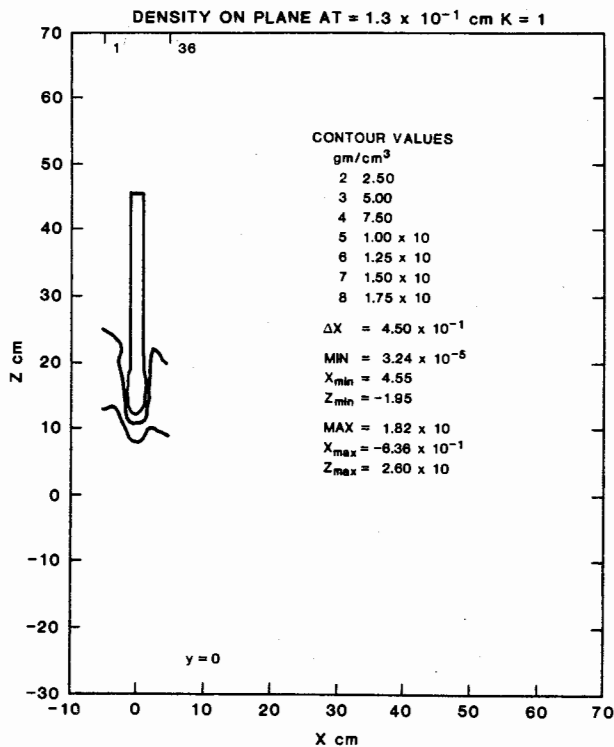
TIME 75.000 μ s CYCLE 263 PROBLEM 100.0

View (a)



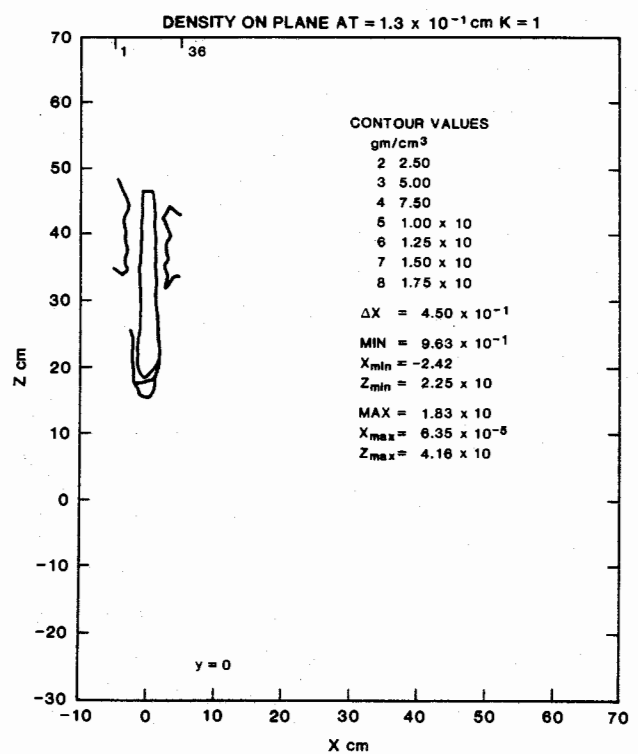
TIME 200.000 μ s CYCLE 696 PROBLEM 100.01

View (c)



TIME 152.507 μ s CYCLE 531 PROBLEM 100.0

View (b)



TIME 300.000 μ s CYCLE 1041 PROBLEM 100.01

View (d)

Figure 3. Sequential Density Plots After Penetration

INTERNAL DISTRIBUTION ONLY:

1520 D. J. McCloskey
1522 P. P. Stirbis
1530 L. W. Davison
1531 S. L. Thompson
1531 F. J. Zeigler
1533 P. Yarrington
1534 J. R. Asay
1600 R. G. Clem
1650 D. J. Rigali
1651 A. K. Miller
1651 M. W. Sterk
1652 A. C. Bustamante
5341 C. E. Dalton
5341 M. J. Forrestal
5341 G. E. Reis
8024 M. A. Pound
3141 C. M. Ostrander (5)
3151 W. L. Garner

